Discrete Mixing of Nanoliter Drops in Microchannels

Minsoung Rhee[*], Mark A. Burns[*,**]

[*]Department of Chemical Engineering, the University of Michigan
2300 Hayward St. 3074 H.H. Dow Building, Ann Arbor, MI 48109-2136, minsoung@umich.edu
[**]Department of Biomedical Engineering, the University of Michigan
2200 Bonisteel Blvd, Ann Arbor, MI 48109-2099, maburns@umich.edu

ABSTRACT

The drop mixing occurs in three different regimes (diffusion, dispersion, and convection-dominated) depending on various operational parameters collectively expressed by the Péclet number ($Pe = U_d \cdot d/D$) and the drop dimensions. Introducing the modified Péclet number ($Pe^* = Pe \cdot d/L$), we present asymptotic curves to predict the mixing time and the required drop displacement distance for mixing at a given Pe^*. COMSOL simulations and on-chip experiments were performed to verify the theoretical limits. The simulated mixing results for the three different regimes show distinctly different mixing behaviors as predicted in the theoretical modeling. In our experimental work, we used a PDMS microchannel with a unique membrane air bypass valve (MBV) to precisely control the mixing and merging site. Finally, we show that experimental, simulation, and theoretical results all agree and confirm that mixing can occur in fractions of a second to hours. The presented work guides understanding of discrete drop mixing and show that efficient mixing in microfluidic systems can be achieved in a simple mixing scheme.

Keywords: drop mixing, micromixer, lab-on-a-chip

1 INTRODUCTION

In many microfluidic applications, rapid mixing is a major challenge because the time for this diffusive mixing often exceeds processing times for other steps. This slow transport time scale may be a bottleneck for many high-throughput microfluidic tests and has negative implications on microfluidic device fabrication [1-3].

A variety of micromixers have been described in the literature [4] to accelerate mixing. Micromixers can be categorized as passive or active. Passive micromixers rely on geometrical properties of channel shape to induce complicated fluid-particle trajectories and thus greatly enhance mixing. The mixing process in these systems is dominated by diffusion or chaotic advection. Various passive mixers that have been reported include techniques such as hydrodynamic focusing [5], packed-bed mixing [6], multi-lamination [7], injection [8], chaotic advection [9], and droplet mixing [10]. Passive micromixers often require deliberate fabrication of channel geometry, but do not require external actuators. In contrast, active micromixers accommodate one or more of the externally-generated disturbance forces.

Mixing in microfluidic systems occurs not only in a continuous flow but also between two drops in a discrete or batch operation. While most micromixers are used in continuous-flow systems, several studies have been reported on microfluidic mixing in batch systems [3, 11]. As opposed to continuous-flow systems, mixing in batch systems can be enhanced by convection [12]. During the course of drop transportation, the internal circulation streamlines of liquid in a moving discrete drop [13] allows convective mixing as well as molecular diffusion.

2 THEORETICAL MODELING

We assume a pressure driven flow in a slit-type microchannel (w>>d) (Fig. 1a). Because of this aspect ratio, we can further assume that the mass transfer is independent of the channel width direction (z-axis) and thus use a two-dimensional model. The liquid inside a discrete drop moving in a microchannel experiences internal circulation within itself [13] (Fig. 1b). The striations produced by the circulation create diffusion distances that are a fraction of the channel depth thus greatly reducing diffusion times.

When the combined sequential drops move along the channel, the solute can either be transported convectively or diffusively to a region of different concentration. The governing transport equation for the slit-channel model is simplified as follows [12].

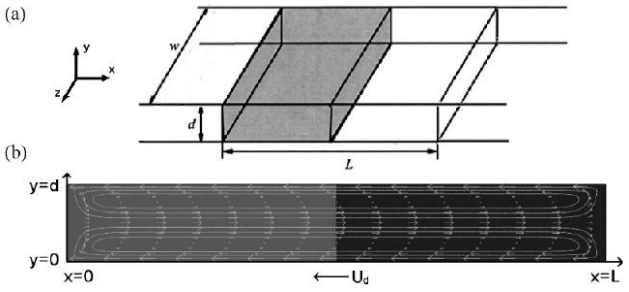

Figure 1. Discrete Drop Mixing Model. (a) An axially-arranged discrete drop placed in a slit-type microchannel (b) Internal circulation streamlines. The arrows represent the velocity vectors in the x-y plane.

NSTI-Nanotech 2008, www.nsti.org, ISBN 978-1-4200-8505-1 Vol. 3

$$\frac{\partial c}{\partial t}+U(y)\frac{\partial c}{\partial x}=D\left(\frac{\partial^2 c}{\partial x^2}+\frac{\partial^2 c}{\partial y^2}\right) \quad (1)$$

where $U(y)=0.5U_d\left(1-3\left(\frac{y}{d/2}\right)^2\right)$. (2)

3 RESULTS AND DISCUSSION

3.1 Analytical Solutions

The relative importance of convection to diffusion in mass transport is usually expressed as the Péclet number (Pe), where $Pe=U_d d/D$, which is useful to estimate the mixing time. Although a direct analytical solution to the Eq (1) is not available, the equation can be further simplified to estimate the mixing time when the Péclet number is within certain ranges: (i) when Pe is very small, (ii) when Pe is in an intermediate range, and (iii) when Pe is very large.

Diffusion-dominated Mixing.

When the Péclet number is very small (Pe<<1), convection is very slow compared to diffusion and the solute is transported entirely by diffusion. We assume that the y-axis dependence can be neglected and Eq (1) can be simplified and gives a cosine series solution as follows.

$$\theta_1=\frac{1}{L/2}\int_0^{L/2}\theta(x)dx=0.5+\sum_{\substack{n=1\\ odd}}^{\infty}\frac{4}{(n\pi)^2}\exp\left(-\frac{t}{\tau_L}n^2\pi^2\right) \quad (3)$$

$$\theta_2=\frac{1}{L/2}\int_{L/2}^{L}\theta(x)dx=0.5-\sum_{\substack{n=1\\ odd}}^{\infty}\frac{4}{(n\pi)^2}\exp\left(-\frac{t}{\tau_L}n^2\pi^2\right). \quad (4)$$

where $\tau_L=L^2/D$ and θ is the average dimensionless concentration of the left(1) or right(2) domain in Figure 1c, which is a function of the axial position (x) and time (t).

We assume that the effective mixing time t_{mix} is the time that elapsed until the drop is mixed 90% (θ_1<0.55 and θ_2>0.45, respectively). The shortest t_{mix} that satisfies the above conditions is given by $0.21\tau_L$. The mixing time can be further non-dimensionalized with the reference diffusion time $\tau_D=d^2/D$ and the aspect ratio, ε=L/d.

$$\tau_{mix}=\frac{t_{mix}}{\tau_D}=0.21\frac{\tau_L}{\tau_D}=0.21\frac{L^2/D}{d^2/D}=0.21\varepsilon^2 \quad (5)$$

In Figure 2a, the diffusion-dominated mixing time is plotted at various drop aspect ratios. Note that the mixing time is neither dependent on the drop velocity nor Pe but is proportional to the square of the drop aspect ratio, L/d. Since the mass transport is caused entirely by diffusion, the mixing time becomes independent of Pe, but as the drop size gets longer, the mixing time increases because the length for diffusion along the drop increases.

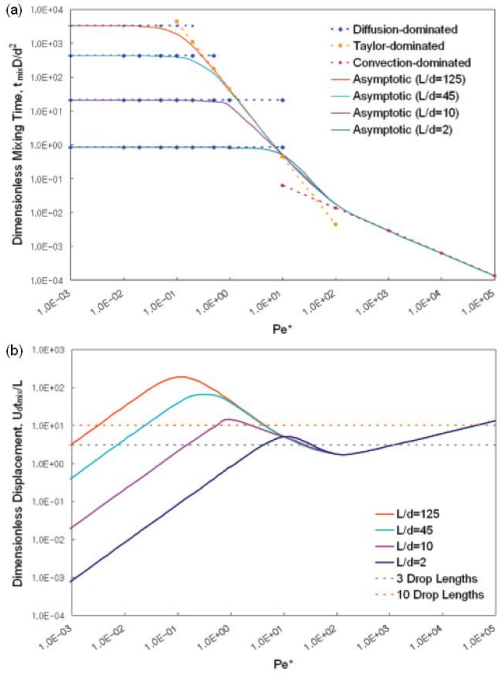

Figure 2. Analytical Quantification of Mixing. (a) Three different mixing regimes and asymptotic curves for mixing time at various drop aspect ratios. (b) Asymptotic curves for drop displacement required for mixing at various aspect ratios.

Dispersion-dominated Mixing.

For $1<<Pe<\pi^2\varepsilon$, the mixing can be described by Taylor dispersion. For slit-type channels, the Taylor dispersion coefficient, D_{TD}, is given by the following relationship [14]:

$$D_{TD}=\frac{U_d^2 d^2}{210D}=\frac{1}{210}Pe^2 D. \quad (6)$$

The diffusion coefficient in the right-hand side of Eq (1) can be replaced with D_{TD} without significant loss of accuracy because Pe is much greater than the unity. The replacement of D results in a mixing time of

$$\tau_{mix}=\frac{t_{mix}}{\tau_D}=0.21\frac{\tau_{TD}}{\tau_D}=0.21\frac{L^2/D_{TD}}{d^2/D}=44.1\frac{\varepsilon^2}{Pe^2} \quad (7)$$

When the transport is dominated by Taylor dispersion, the mixing time is proportional to the inverse square of Pe, indicating that the mixing is enhanced as the drop velocity increases or the drop aspect ratio decreases.

To better explain the correlation between mixing and the aspect ratio, a modified Péclet number has been suggested. The main idea behind this modification is that when convective mixing occurs, convection and diffusion usually develop in different directions. Thus, for a system with a high aspect ratio, the Péclet number provides

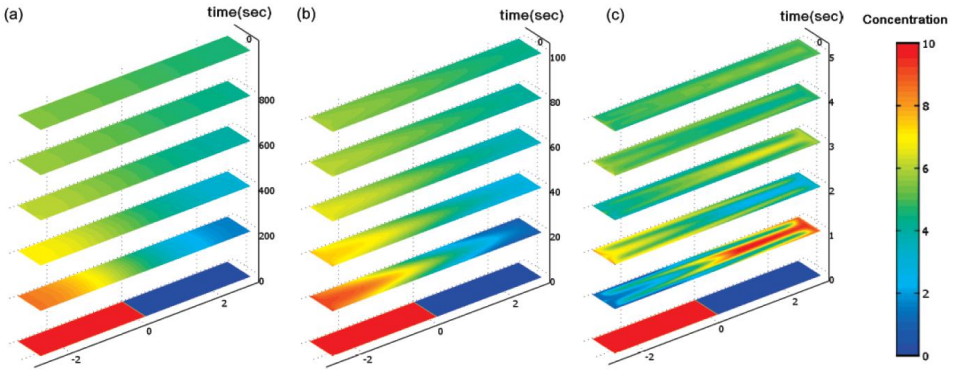

Figure 3. COMSOL 2D Simulation. Concentration variation in time from bottom to top in a straight channel (ε=7) for (a) Pe*=0.4, (b) Pe*=6, and (c) Pe*=132

insufficient information about the importance of convection and diffusion. The modified Péclet number is defined by,

$$Pe^* = \frac{\text{diffusive time scale}}{\text{convective time scale}} = \frac{d^2/D}{L/U_d} = \frac{Pe}{\varepsilon}. \quad (8)$$

With Pe*, Eq (15) can be now rewritten by

$$\tau_{mix} = \frac{t_{mix}}{\tau_D} = 44.1(Pe^*)^{-2}. \quad (9)$$

and the dependency of the dispersion-dominated mixing time on Pe* can be seen in Figure 2a. The mixing time is independent of the aspect ratio as a function of Pe*.

Convection-dominated Mixing.

When the drop velocity is sufficiently fast (Pe*>> π^2), multiple layers develop due to the internal circulatory flow. After a certain mixing time t_C, the drop travels N= $U_d t_C/L$ drop lengths and makes n=N/3=$U_d t_C/3L$ internal circulations. The internal circulations cause the solute layers to fold over themselves every half circulation, and thus the number of foldings (N_F) correspond to N_F=2n or N_F=2N/3. Such circulations would create 2.25N_F or 9N_F/4 layers. Thus, the number of layers (N_L) can be calculated as a function of the number of drop lengths that the drop travels using the equation

$$N_L = \frac{9}{4}N_F = \frac{3}{2}N. \quad (10)$$

Mixing occurs when the solutes diffuse between two adjacent layers. When there are N_L layers within the depth d, the interlayer distance, s, is approximated as s=d/2N_L=d/3N. If the interlayering continues until the solute diffuses to complete mixing (90%), the radial diffusion reference timescale 0.21s^2/D must be balanced with t_C (i.e., t_C=0.21s^2/D). The mixing time is then calculated as follows:

$$\tau_{mix} = \frac{t_{mix}}{\tau_D} = \frac{t_C}{\tau_D} = (0.21)^{1/3}\left(\frac{1}{3}\right)^{2/3}\left(\frac{L/U_d}{d^2/D}\right)^{2/3} = 0.286(Pe^*)^{-2/3} \quad (11)$$

Drop Displacement Required for Mixing.

Another problem of great relevance to experimentalists is to find the optimal geometry to give the lowest possible mixing time. A dimensionless displacement for mixing, λ_{mix}, can be defined as the ratio of the displacement versus the drop length,

$$\lambda_{mix} = \frac{U_d t_{mix}}{L} = \tau_{mix}\left(\frac{d^2/D}{L/U_d}\right) = \tau_{mix}(Pe^*). \quad (12)$$

Figure 2b plots the estimated displacement required for mixing. When Pe* is very small, the displacement is proportional to Pe* or the drop velocity, because the drop is constantly moving during slow diffusive mixing. In contrast, the required displacement in the Taylor dispersion-dominated mixing regime (π^2/ε<<Pe*<< π^2) decreases with Pe*, since the convective flow greatly improves mixing efficiency. Finally, when the flow is too fast (Pe*>> π^2), the required displacement increases algebraically with Pe*, although the mixing time decreases.

3.2 Drop Mixing Simulations

Computer simulations were performed to confirm the theoretical modeling results. In Figure 1b, the upper and lower walls move in the negative x-direction with the

Figure 4. Simulated interlayering progress for ε=7 and Pe*=2000.

NSTI-Nanotech 2008, www.nsti.org, ISBN 978-1-4200-8505-1 Vol. 3

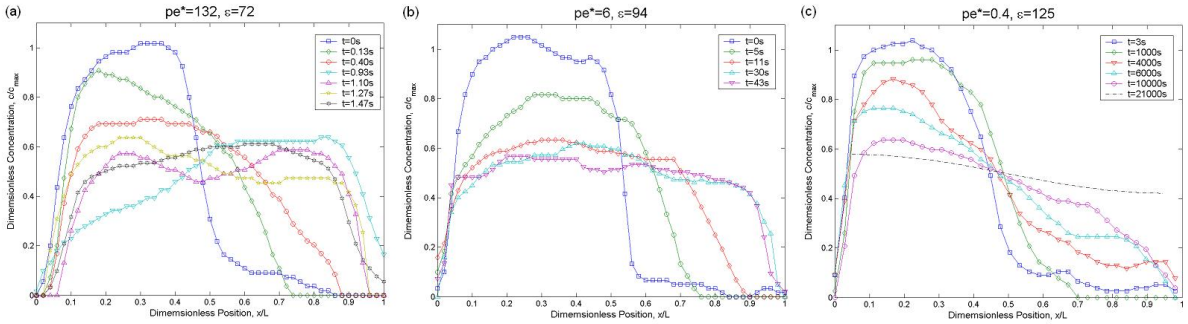

Figure 5. Average concentration profile at different times. (a) Convective Mixing Progress (Pe*=132). (b) Dispersive Mixing Progress (Pe*=6). (c) Diffusive Mixing Progress (Pe*=0.4).

velocity -U_d. This motion simulates a drop moving through a straight channel at the velocity of U_d. Combined with the no-slip boundary conditions at the front and back ends of the drop, the internal circulatory flows inside the drop were simulated.

In Figure 3, the mixing progress in a straight channel for (a) Pe*=0.4, (b) Pe*=6, and (c) Pe*=132 were simulated, respectively. Note that the mixing for Pe*=0.4 and Pe*=6 is dominated by diffusion and Taylor-dispersion, respectively. No apparent sign of convective transport by internal circulation is observed. In contrast, interlayering is observed in Figure 3c indicating that convection has a significant role in mixing for Pe*=132. Figure 4 illustrates the simulated interlayering progress for Pe*=2000. The layers remain for an extended time because the convective transport is much faster than the diffusive transport.

3.3 Experimental Verification

In experiments, one can alter the mixing condition (Pe*) by controlling the drop velocity. Figure 5a shows the experimental mixing progress at a high Pe* (~132), starting from the initial state when the two drops fuse and an interface develops, to the state of complete mixing. Note that the merged drop rapidly mixes within a few seconds.

In the intermediate range of Pe*(~6) (Fig. 5b), however, the mixing occurs more slowly. When Pe* is small (~0.4) the merged drop has been displaced 63 mm for ~10000 seconds back and forth along the channel but the mixing was quite incomplete (Fig. 5c). In Figure 6, we show that our experimental results are in good agreement with the theoretical modeling as well as simulation results.

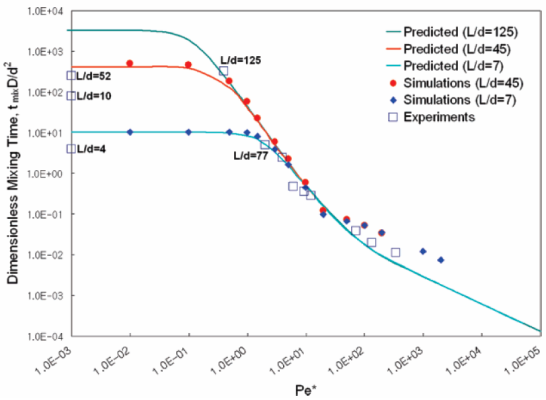

Figure 6. Mixing time comparison among theoretical predictions, simulations, and experimental results.

ACKNOWLEDGMENT

The authors would like to acknowledge the National Institutes of Health (P01-HG001984, R01-AI049541, R01-GM-37006-17) for partial funding of this work.

REFERENCES

[1] Song, H.; Chen, D. L.; Ismagilov, R. F. *Angew. Chem. Int. Ed. Engl*. **2006**, *45*, 7336-7356.
[2] Burns, M. A. *Science*. **2002**, *296*, 1818-1819
[3] Burns, M. A. *et al. Science* **1998**, *282* (5388), 484-487
[4] Nguyen, N.; Wu, Z. *J. Micromech. Microeng*. **2005**, *15*, R1–R16
[5] Knight, J. B.; Vishwanath, A.; Brody, J. P.; Austin, R. H. *Phys. Rev. Lett.*, **80**, 3863–3866.
[6] Lin, Y.; Gerfen, G. J.; Rousseau, D. L.; Yeh, S. R. *Anal. Chem*. **2003**, *75*, 5381–5386.
[7] Schwesinger, N.; Frank, T.; Wurmus, H. *J Micromech. Microeng*. **1996**, *6*, 99–102.
[8] Okkels, F.; Tabling, P. *Phys. Rev. Lett*. **2004**, *92*, 038301.
[9] Bertsch, A.; Heimgartner, S.; Cousseau, P.; Renaud, P. *Lab Chip*. **2001**, *1*, 56–60.
[10] Burns, J. C.; Ramshaw, C. *Lab Chip*, **2001**, *1*, 10–15.
[11] Thorsen, T. ; Maerkl, S. J.; Quake, S. R. *Science*, **2002,** *298***,** 580-584.
[12] Handique, K.; Burns, M. A. *J. Micromech. Microeng*. **2001**, *11*, 548-554.
[13] Duda, J. L.; Vrentas, J. S. *J. Fluid Mech*. **1971**, *45*, 247–260.
[14] Taylor, G., *Proc. R. Soc. London, Ser*. A. **1953**, *219*, 186-203.